Hybrid Control of Formations of Robots

R. Fierro, A. K. Das, V. Kumar, and J. P. Ostrowski

GRASP Laboratory – University of Pennsylvania, Philadelphia, PA, 19104, USA
{rfierro, aveek, kumar, jpo}@grasp.cis.upenn.edu

Abstract

We describe a framework for controlling a group of nonholonomic mobile robots equipped with range sensors. The vehicles are required to follow a prescribed trajectory while maintaining a desired formation. By using the leader-following approach, we formulate the formation control problem as a hybrid (mode switching) control system. We then develop a decision module that allows the robots to automatically switch between continuous-state control laws to achieve a desired formation shape. The stability properties of the closed-loop hybrid system are studied using Lyapunov theory. We do not use explicit communication between robots; instead we integrate optimal estimation techniques with nonlinear controllers. Simulation and experimental results verify the validity of our approach.

1 Introduction

Research activity in multi-robotic systems has increased substantially in the last few years. Topics include cooperative manipulation [9], multi-robot motion planning, collaborative mapping and exploration [2], software architectures for multi-robotic systems [12], and formation control [6]. Areas of application include, undersea and space exploration, surveillance, target acquisition, and service robotics for mention just a few. Researchers in multi-robotic systems are facing new challenges and open issues that require deeper investigation. For instance, we need to address stability and robustness of multi-agent hybrid systems and develop the methodology and the software that will enable robots to exhibit deliberative and reactive behaviors, and to learn and adapt to unstructured, dynamic environments and new tasks, while providing performance guarantees.

This work considers the problem of formation control. Formation control of multiple autonomous vehicles arises in many scenarios of current interest. For example, in military applications and intelligent vehicle highway systems (IVHS) vehicles need to maneuver while keeping a prescribed formation. To be more specific, we consider a team of n nonholonomic mobile robots that are required to follow a prescribed trajectory while maintaining a desired formation. A robot designated as the *reference* robot follows a trajectory generated by a high-level planner. By using the *leader-following* approach, we split the formation control problem into:

Continuous-state robot control: Control algorithms are designed based on I/O feedback linearization. Each robot can maintain a prescribed separation and bearing from its adjacent neighbors. Explicit inter-robot communication is avoided by using optimal estimation techniques.

Discrete-state formation control: A desired formation is achieved by sequential composition of basic maneuvers (control algorithms). Switching rules are formulated based on sensor constraints.

The paper is organized as follows. In section 2, we provide some mathematical preliminaries and present a brief description of the set of controllers we use in our work. The sequential composition of behaviors and the formation switching strategy are addressed in section 3. Section 4 presents simulation and experimental results. Finally, some concluding remarks and future work ideas are given in section 5.

2 Formation Control

In this section, we describe a formation of n robots as a tuple $\mathcal{F} = (r,\ \mathcal{H})$ where r is a set of variables describing the relative positions of the robots with respect to the reference robot, and $\mathcal{H}$ is a formation graph describing the control strategy used by each robot. Thus, $\mathcal{F}$ is a dynamical system evolving in continuous-time on the interval $T = [t_0,\ t_N] \subset \mathbb{R}^+$. The configuration space for $\mathcal{F}$ is $\mathcal{C} = SE(2)^n$.

A formation change can be accomplished by using the compositional control approach introduced in [3]. The main idea is to define a set of controllers $U = \{\xi_1, \ldots, \xi_p\}$ for each robot. Let Φ_j and Ω_j be the domain and goal of controller ξ_j, respectively. It is said that controller ξ_i *prepares* controller ξ_k (denoted $\xi_i \succ \xi_k$) if $\Omega_i \subseteq \Phi_k$. For a given suitably designed set of controllers U, a switching strategy can be found such that the team of robots achieves a

desired formation $\mathcal{F}^d$ from any initial formation $\mathcal{F}_0$. Thus, the control problem of formations of robots can be formulated as a hybrid system whose continuous dynamics change in a *controlled* fashion [7]. Let $g \in SE(2)$ denote the reference robot's trajectory. The kinematics of the nonholonomic i-robot are given by

$$\dot{x}_i = v_i \cos\theta_i, \qquad \dot{y}_i = v_i \sin\theta_i, \qquad \dot{\theta}_i = \omega_i \quad (1)$$

In the next subsections we describe briefly three controllers used for formation control purposes. The first two are adopted from [6]. We derived here a third controller that takes into account obstacles.

2.1 Separation Bearing Control

In the *S*eparation *B*earing *C*ontroller (denoted $SB_{ij}C$), robot R_j follows R_i with a desired separation l_{ij}^d and a desired relative bearing ψ_{ij}^d, see Figure 1. The control velocities for the follower are given

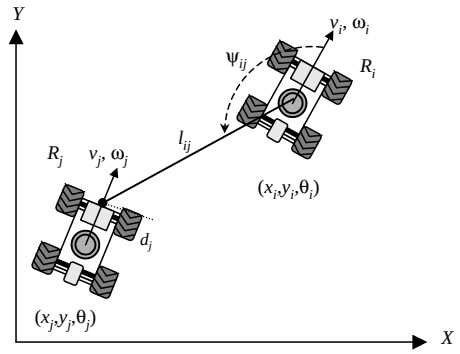

Figure 1: The *S*eparation *B*earing *C*ontroller.

by

$$v_j = s_{ij}\cos\gamma_{ij} - l_{ij}\sin\gamma_{ij}(b_{ij}+\omega_i) + v_i\cos(\theta_i-\theta_j) \quad (2)$$

$$\omega_j = \frac{s_{ij}\sin\gamma_{ij} + l_{ij}\cos\gamma_{ij}(b_{ij}+\omega_i) + v_i\sin(\theta_i-\theta_j)}{d} \quad (3)$$

where

$$\begin{aligned} \gamma_{ij} &= \theta_i + \psi_{ij} - \theta j, \quad s_{ij} = k_1(l_{ij}^d - l_{ij}), \\ b_{ij} &= k_2(\psi_{ij}^d - \psi_{ij}), \quad k_1, k_2 > 0 \end{aligned} \quad (4)$$

The closed-loop linearized system becomes

$$\dot{l}_{ij} = k_1(l_{ij}^d - l_{ij}), \quad \dot{\psi}_{ij} = k_2(\psi_{ij}^d - \psi_{ij}), \quad \dot{\theta}_j = \omega_j \quad (5)$$

2.2 Separation Separation Control

In the *S*eparation *S*eparation *C*ontroller (denoted $S_{ik}S_{jk}C$), robot R_k follows R_i and R_j with desired separations l_{ik}^d and l_{jk}^d, respectively. See Figure 2. In this case, the control velocities for the follower become

$$\begin{aligned} v_k &= \frac{s_{ik}\sin\gamma_{jk} - s_{jk}\sin\gamma_{ik} + v_i\cos\psi_{ik}\sin\gamma_{jk}}{\sin(\gamma_{jk}-\gamma_{ik})} \\ &\quad - \frac{v_j\cos\psi_{jk}\sin\gamma_{ik}}{\sin(\gamma_{jk}-\gamma_{ik})} \end{aligned} \quad (6)$$

$$\begin{aligned} \omega_k &= \frac{-s_{ik}\cos\gamma_{jk} + s_{jk}\cos\gamma_{ik} - v_i\cos\psi_{ik}\cos\gamma_{jk}}{d\sin(\gamma_{jk}-\gamma_{ik})} \\ &\quad + \frac{v_j\cos\psi_{jk}\cos\gamma_{ik}}{d\sin(\gamma_{jk}-\gamma_{ik})} \end{aligned} \quad (7)$$

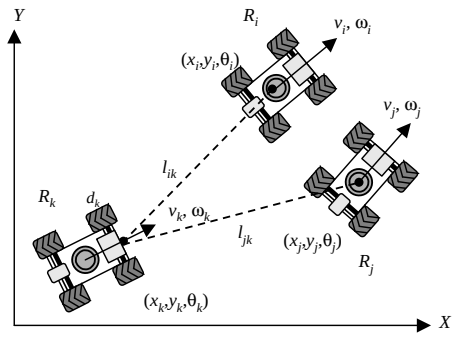

Figure 2: The *S*eparation *S*eparation *C*ontroller.

The closed-loop linearized system is

$$\dot{l}_{ik} = k_1(l_{ik}^d - l_{ik}), \quad \dot{l}_{jk} = k_1(l_{jk}^d - l_{jk}), \quad \dot{\theta}_k = \omega_k \quad (8)$$

2.3 Separation Distance-To-Obstacle Control

In the *S*eparation *D*istance-To-*O*bstacle *C*ontroller (denoted SD_OC), the outputs of interest are the separation l_{ij} between the follower robot and leader, and the distance δ from an obstacle to the follower. We define a virtual robot R_0, as shown in Figure 3, which moves on the obstacle's boundary with linear velocity v_0 and orientation θ_0. For this case the kinematics of R_j become

$$\begin{aligned} \gamma_{0j} &= \theta_0 - \theta_j \\ \dot{l}_{ij} &= v_j\cos\gamma_{ij} - v_i\cos\psi_{ij} + d\omega_j\sin\gamma_{ij} \\ \dot{\delta} &= v_j\sin\gamma_{0j} - d\omega_j\cos\gamma_{0j} \\ \dot{\theta}_j &= \omega_j \end{aligned} \quad (9)$$

where γ_{ij} is given in (4) and $\delta = \inf\|x_j - x_{Obs}\|$. Feedback I/O linearization is possible as long as

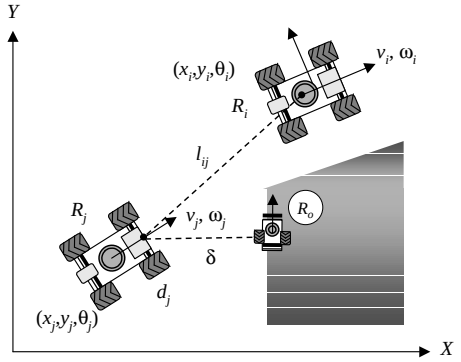

Figure 3: *S*eparation *D*istance–To–*O*bstacle *C*ontrol.

$d\cos(\gamma_{0j} - \gamma_{ij}) \neq 0$, *i.e.*, the controller is not defined whether $d = 0$ or $\gamma_{0j} - \gamma_{ij} = \pm k\frac{\pi}{2}$. The latter occurs when vectors $\vec{\delta}$ and $\vec{l}_{ij}$ are collinear. The velocity inputs for R_j are given by

$$v_j = \frac{s_{ij}\cos\gamma_{oj} + s_{oj}\sin\gamma_{ij} + v_i\cos\psi_{ij}\cos\gamma_{oj}}{\cos(\gamma_{oj} - \gamma_{ij})} \tag{10}$$

$$\omega_j = \frac{s_{ij}\sin\gamma_{oj} - s_{oj}\cos\gamma_{ij} + v_i\cos\psi_{ij}\sin\gamma_{oj}}{d\cos(\gamma_{oj} - \gamma_{ij})} \tag{11}$$

Thus, the linearized kinematics become

$$\begin{aligned} \dot{l}_{ij} &= k_1(l_{ij}^d - l_{ij}) \equiv s_{ij} \\ \dot{\delta} &= k_0(\delta_0 - \delta) \equiv s_{0j} \\ \dot{\theta}_j &= \omega_j \end{aligned} \tag{12}$$

where k_1, k_0 are positive controller gains, and δ_0, l_{ij}^d are desired distances to the obstacle and reference robot, respectively.

2.4 Stability Analysis

In this section, we provide stability results for the *SBC* and *SSC*, respectively. Proofs are omitted here due to space constraints. Details are discovered in [8].

Theorem 2.1 *Assume that the reference linear velocity along the trajectory $g(t) \in SE(2)$ is lower bounded i.e., $v_i > V_{\min} > 0$, the reference angular velocity is also bounded i.e., $\|\omega_i\| < W_{\max}$, and the initial relative orientation $\|\theta_i(t_0) - \theta_j(t_0)\| < c_1\pi$ for some positive constant $c_1 < 1$. If the control velocities (2)–(3) are applied to R_j, then system (5) is stable and the output system error of the linearized system converges to zero exponentially.*

□

Theorem 2.2 *Assume that the reference linear velocity along the trajectory $g(t) \in SE(2)$ is lower bounded i.e., $v_i > V_{\min} > 0$, the reference angular velocity is also bounded i.e., $\|\omega_i\| < W_{max}$, the relative velocity $\delta_v \equiv v_i - v_j$ and orientation $\delta_\theta \equiv \theta_i - \theta_j$ are bounded by small positive numbers ε_1, ε_2, and the initial relative orientation $\|\theta_i(t_0) - \theta_k(t_0)\| < c_2\pi$ for some positive constant $c_2 < 1$. If the control velocities (6)–(7) are applied to R_k, then system (8) is stable and the output system error of the linearized system converges to zero exponentially.*

□

Remarks The two output variables in (5) and (8) converge to the desired values arbitrarily fast (depending on k_1 and k_2). The main difficulty arises in considering the internal dynamics, for instance θ_k in (8), which depends on the controlled velocity ω_k. The orientation error can be expressed as

$$\dot{e}_\theta = \omega_i - \omega_k \tag{13}$$

After some work, we have

$$\dot{e}_\theta = -\frac{v_i}{d}\sin e_\theta + \eta(\boldsymbol{u}, e_\theta) \tag{14}$$

where $\boldsymbol{u}$ is a vector that depends on the output system error and reference angular velocity ω_i. $\eta(\cdot)$ is a nonvanishing perturbation for the *nominal* system in (14) which is (locally) exponentially stable. By using stability of perturbed systems [10], it can be shown that system (14) is stable, thus the stability results in Theorems 2.1 and 2.2 follow.

3 A 3-Robot Formation Control Case

We illustrate our approach using three nonholonomic mobile robots $R_{1,2,3}$ moving in an obstacle-free environment. First, R_1, the *reference* robot, follows a given trajectory $g(t) \in SE(2)$. Second, R_2, the *leader* robot, follows R_1 with $SB_{12}C$. Finally, R_3, the *follower*, has to maintain a specified distance from R_1 and R_2, *i.e.*, $S_{13}S_{23}C$. However, R_3 may change its control behavior depending on its position with respect to R_1 and R_2. Thus, for any arbitrary initial configuration, R_3 may follow R_1 or R_2 with $SB_{13}C$ or $SB_{23}C$. Eventually, R_3 will switch between different control behaviors in order to reach the desired formation. The palette of controllers becomes $U = \{U_2 \cup U_3\}$, and $U_2 = \{SB_{12}C\}$, $U_3 = \{SB_{13}C, SB_{23}C, S_{13}S_{23}C\}$. The finite set of discrete formation modes $Q = \{q_1, q_2, q_3\}$ is illustrated in Figure 4.

Assume that $q_3 \in Q$ is the desired formation $\mathcal{F}^d$, and $\mathcal{F}_0$ is an initial formation. The hybrid system is

designed using the compositional control approach outlined in section 2. Let $\{\Phi_1, \Omega_1\}$, $\{\Phi_2, \Omega_2\}$, and $\{\Phi_3, \Omega_3\}$ be the {domain, goal} of $SB_{13}C$, $SB_{23}C$, $S_{13}S_{23}C$, respectively. We design the controllers such that $\Omega_1 \subseteq \Phi_3$ and $\Omega_2 \subseteq \Phi_3$, then $SB_{13}C \succ S_{13}S_{23}C$, similarly $SB_{23}C \succ S_{13}S_{23}C$. In the next section, we formalize this approach by using Lyapunov stability theory to show that under reasonable assumptions $\mathcal{F}^d$ is achieved in a stable manner from any $\mathcal{F}_0$.

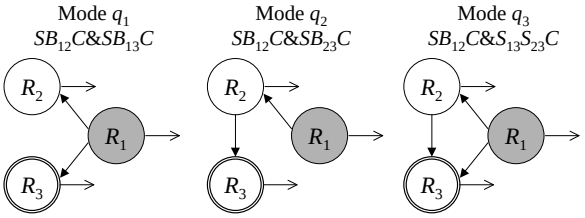

Figure 4: Formation modes for the 3-Robot case.

The closed-loop formation modes are given by
Mode q_1: $SB_{12}C\&SB_{13}C$

$$\begin{aligned} \dot{l}_{12} &= k_1(l_{12}^d - l_{12}) & \dot{l}_{13} &= k_1(l_{13}^d - l_{13}) \\ \dot{\psi}_{12} &= k_2(\psi_{12}^d - \psi_{12}) & \dot{\psi}_{13} &= k_2(\psi_{13}^d - \psi_{13}) \\ \dot{\theta}_2 &= \omega_2 & \dot{\theta}_3 &= \omega_3 \end{aligned} \quad (15)$$

Mode q_2: $SB_{12}C\&SB_{23}C$

$$\begin{aligned} \dot{l}_{12} &= k_1(l_{12}^d - l_{12}) & \dot{l}_{23} &= k_1(l_{23}^d - l_{23}) \\ \dot{\psi}_{12} &= k_2(\psi_{12}^d - \psi_{12}) & \dot{\psi}_{23} &= k_2(\psi_{23}^d - \psi_{23}) \\ \dot{\theta}_2 &= \omega_2 & \dot{\theta}_3 &= \omega_3 \end{aligned} \quad (16)$$

Mode q_3: $SB_{12}C\&S_{13}S_{23}C$

$$\begin{aligned} \dot{l}_{12} &= k_1(l_{12}^d - l_{12}) & \dot{l}_{13} &= k_1(l_{13}^d - l_{13}) \\ \dot{\psi}_{12} &= k_2(\psi_{12}^d - \psi_{12}) & \dot{l}_{23} &= k_1(l_{23}^d - l_{23}) \\ \dot{\theta}_2 &= \omega_2 & \dot{\theta}_3 &= \omega_3 \end{aligned} \quad (17)$$

Actually, the gains k_1 and k_2 can be different in each mode. For simplicity, we use the same values in our simulations and experiments. Let the system error be defined as

$$\begin{aligned} e_1 &= l_{13}^d - l_{13}, \quad e_2 = \psi_{13}^d - \psi_{13}, \quad e_3 = \theta_1 - \theta_3 \\ e_4 &= l_{23}^d - l_{23}, \quad e_5 = \psi_{23}^d - \psi_{23}, \quad e_6 = \theta_2 - \theta_3 \\ e_7 &= l_{12}^d - l_{12}, \quad e_8 = \psi_{12}^d - \psi_{12}, \quad e_9 = \theta_1 - \theta_2 \end{aligned}$$

For every mode, we have $e_{ijk} \equiv [e_i\ e_j\ e_k]^T$ where e_{ij} and e_k correspond to the outputs of interest and the internal dynamics, respectively. Moreover, if the assumptions in theorems 2.1 and 2.2 hold, then each formation mode (15)–(17) is stable. Now, we need to prove that for a given switching strategy S_w, the hybrid system is stable, *i.e.*, given any initial formation $\mathcal{F}_0$, a desired $\mathcal{F}^d$ is achieved in finite time.

3.1 Switching Strategy

Our robots are equipped with an on-board omnidirectional vision system. The sensor constraints determine the switching sequence S_w. R_3 may detect R_1, R_2 or both. In some cases, neither R_1 nor R_2 are within the field of view of R_3. Figure 5 depicts the switching boundaries in Cartesian space. Notice the triangle inequality $l_{ik} + l_{jk} > l_{ij}$ should be satisfied. If R_i with $i = 1, 2, 3$ were collinear, SSC would not be defined, then a SBC should be utilized.

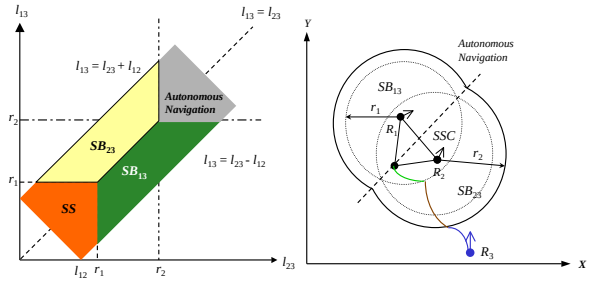

Figure 5: Switching boundaries based on sensor constraints.

The formation control objective is to drive R_3 to a region where it can detect both R_1 and R_2. Thus, the switching control strategy for R_3 can be summarized as follows

$$\begin{aligned} &\text{If } (l_{13} < l_{23})\&(l_{23} > r_1)\&(l_{13} < r_2) \text{ Then } SB_{13}C \\ &\text{If } (l_{13} > l_{23})\&(l_{13} > r_1)\&(l_{23} < r_2) \text{ Then } SB_{23}C \\ &\text{If } (l_{13} < r_1)\&(l_{23} < r_1) \text{ Then } S_{13}S_{23}C \\ &\text{If } (l_{13} > r_2)\&(l_{23} > r_2) \text{ Then } AutonNavig \end{aligned}$$

3.2 Stability Analysis

Since a palette of controllers and a switching strategy are given, we need to *verify* that the hybrid system is stable provided that each mode shares a common equilibrium point $\boldsymbol{x}_0 \in \Omega_3$. One way to solve this verification problem is to find a common Lyapunov function, thus the switched system is stable for any arbitrary fast switching sequence. This is in general a difficult task. A number of approaches have been proposed in the literature to confront this problem (see [11] and the references therein). In our 3-robot formation example, it turns out that under some reasonable assumptions, there may exist a common Lyapunov function. Therefore, the equilibrium point is stable, and the system error of the desired formation mode converges to zero. However, the property of exponential convergence is lost in the switching process. Let $\bar{V}_3(\boldsymbol{e}) = V_3 + V_{12}$ be a Lyapunov function candidate for the desired formation

$\mathcal{F}_3$ in (17), and

$$V_3 = \frac{1}{2}\left[e_1^2 + e_4^2 + e_3^2\right], \quad V_{12} = \frac{1}{2}\left[e_7^2 + e_8^2 + e_9^2\right] \tag{18}$$

V_{12} is a Lyapunov function candidate for subsystem $SB_{12}C$ *i.e.*, R_2 follows R_1 using a separation-bearing controller. If the assumptions in theorem 2.1 are satisfied, then $\dot{V}_{12} \leq 0$. Moreover, if the assumptions in theorem 2.2 are satisfied for subsystem $S_{13}S_{23}C$, then $\dot{V}_3 \leq 0$. We impose an additional constraint on our hybrid system which is R_2 has already reached its equilibrium point. Thus, we only need to consider V_3 in (18) for studying the stability of the switched system $\mathcal{F}_q$. By definition V_3 is a Lyapunov function for $\mathcal{F}_3$. We would like to show that, V_3 is also a Lyapunov function for $\mathcal{F}_1$ and $\mathcal{F}_2$.

Let us consider formation mode $\mathcal{F}_1$. $SB_{13}C$ makes $e_1 \to 0$ and $e_2 \to 0$ exponentially as $t \to \infty$. But we need to show that $\dot{V}_4 = e_4\dot{e}_4 \leq 0$ or $(l_{23}^d - l_{23})\dot{l}_{23} \geq 0$. The main idea here is to pick ψ_{13}^d such that $l_{23} \to l_{23}^d$ as $e_2 \to 0$. Then, we have

$$\psi_{13}^d = \cos^{-1}\left(\frac{{l_{12}^d}^2 + {l_{13}^d}^2 - {l_{23}^d}^2}{2l_{12}^d l_{13}^d}\right) + \psi_{12}^d \tag{19}$$

Using the inequality constraint imposed by the geometry of the problem *i.e.*, $l_{23}^d < l_{12}^d + l_{13}^d$, it is easy to show that $\dot{V}_4 = e_4\dot{e}_4 \leq 0$. Then V_3 is a Lyapunov function for $\mathcal{F}_1$ (similarly for $\mathcal{F}_2$).

It is well known that Lyapunov methods provide conservative stability regions, since we always consider the worst case. Simulation results reveal that the desired formation is achieved even when some of the assumptions discussed here are not satisfied *e.g.*, positions and orientation of R_2 and R_3 are randomly initialized.

4 Simulation and Experimental Results

We simulate the switching strategy outlined in section 3.1. As it can be seen in Figure 6, after some mode switching and obstacle avoidance the 3-Robot system reaches the desired formation. The parameters for simulation are: $v_1 = 0.5$ m/s, R_1: (0, 0, 30°), R_2: (1.5, 0, 0°), R_3: (0.2, 2, 30°), $\omega_1 = 0.1\sin(0.2t)$, $l_{12}^d = l_{13}^d = l_{23}^d = 1$m, and $\psi_{12}^d = 90°$.

4.1 The Experimental Setup

The mobile robots we use for the experiments are shown in Figure 7. Each robot has an onboard omni-directional vision system, a wireless video transmitter, and a battery pack. The receiver (located at the host NT computer) feeds the signal to a frame grabber that is able to capture video at full frame rate (30 Hz.) for image processing.

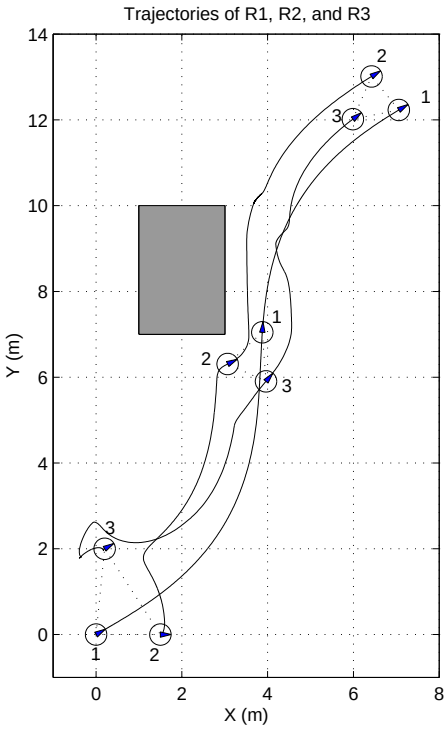

Figure 6: 3-Robot case formation control.

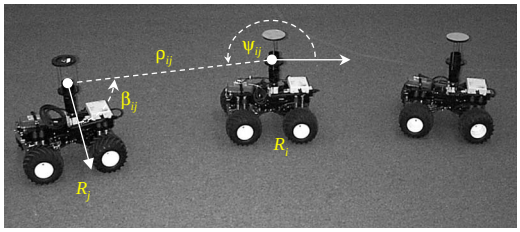

Figure 7: The experimental setup.

The formation controllers described here require reliable estimation of the linear velocity $v_i(t)$ and angular velocity $\omega_i(t)$ of the leader robot R_i, and relative orientation $(\theta_i - \theta_j)$. The omni-directional vision system provides the range ρ_{ij} and the angle β_{ij} of the observed leader. This information is used by the *velocity estimator* that is based on an extended Kalman filter [4]. Control velocities for the follower robot are computed and sent to the driving and steering servomotors. Figure 8 presents experimental results for the separation bearing control (*SBC*). The desired separation and bearing are $l_{ij}^d = 0.6$ m and $\psi_{ij}^d = 180°$, respectively. The reference robot follows a circular path. The robustness of the system is ver-

ified when we manually hold the follower for a few seconds at $t \approx 65$ s.

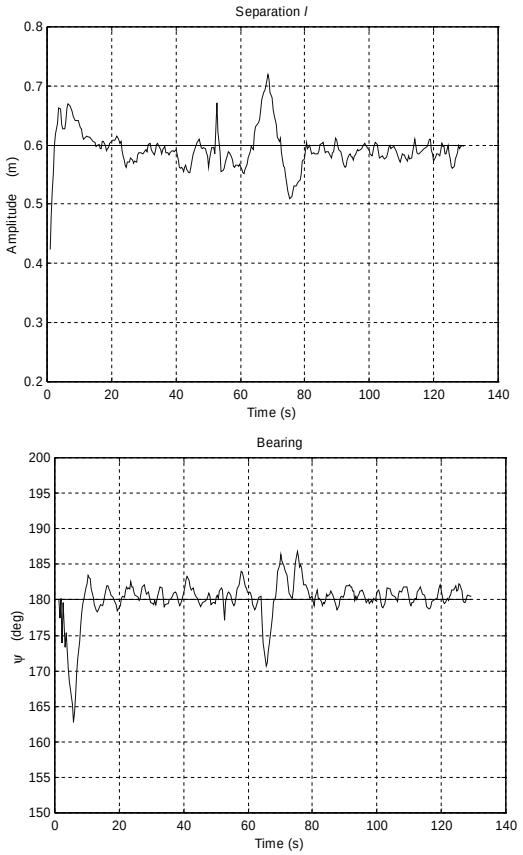

Figure 8: Measured separation and bearing.

Acknowledgements

Research Supported by the DARPA ITO MARS Program, Grant No. 130-1303-4-534328-xxxx-2000-0000

5 Conclusions

In this paper, we have presented a hybrid system approach for formation control. We have designed a suite of controllers for leader following and obstacle avoidance. These individual controllers are sequentially composed in order to achieve a desired formation. Simulation and experimental results verify the validity of our approach. Velocity estimation techniques based on an EKF have been integrated in the closed loop system. Estimation of leader's velocities is required, since there is no inter-agent communication. Experiments are being extended to more complex scenarios where robots need to exhibit a variety of behaviors such as localization, target acquisition, collaborative mapping and formation keeping. The controllers presented in this work are valid for $SE(2)$. Currently, we are investigating similar controllers for $SE(3)$.

References

[1] T. Balch, "Social potentials for scalable multi-robot formations", *Proc. IEEE Int. Conf. Robot & Automat.*, San Francisco, CA, April 2000, pp. 73–80.

[2] W. Burgard, M. Moors, D. Fox, R. Simmons, and S. Thrun, "Collaborative multi-robot exploration," *Proc. IEEE Int. Conf. Robot. and Automat.*, San Francisco, CA, April 2000, pp. 476–481.

[3] R. Burridge, A. Rizzi, and D. Koditschek, "Sequential composition of dynamically dexterous robot behaviors," *Int. J. Robot. Research*, vol. 18, no. 6, pp. 534–555, June 1999.

[4] A. K. Das, R. Fierro, V. Kumar, B. Southall, J. Spletzer, and C. Taylor, "Real-time vision-based control of a nonholonomic mobile robot," *Proc. IEEE Int. Conf. Robot. and Automat.*, Seoul, Korea, May 2001.

[5] A. De Luca, G. Oriolo, and C. Samson, "Feedback control of a nonholonomic car-like robot," in *Robot Motion Planning and Control*, J.-P. Laumond (ed.), London: Springer-Verlag, 1998, pp. 171–253.

[6] J. Desai, J. P. Ostrowski, and V. Kumar, "Controlling formations of multiple mobile robots," *Proc. IEEE Int. Conf. Robot Autom.*, Leuven, Belgium, May 1998, pp. 2864–2869.

[7] R. Fierro and F. L. Lewis, "A framework for hybrid control design," *IEEE Trans. Syst., Man, Cyber.*, vol. 27-A, no. 6, pp. 765–773, Nov. 1997.

[8] R. Fierro, P. Song, A. K. Das, and V. Kumar, "Cooperative control of robot formations," Submitted to Cooperative Control and Optimization Series, Kluwer, 2001.

[9] W. Kang, N. Xi, and A. Sparks, "Formation control of autonomous agents in *3D* workspace," *Proc. IEEE Int. Conf. Robot. Automat.*, San Francisco, CA, April 2000, pp. 1755-1760.

[10] H. K. Khalil, *Nonlinear Systems*, Upper Saddle River, NJ: Prentice Hall, 2^{nd} ed., 1996.

[11] D. Liberzon and A. S. Morse, "Basic problems in stability and design of switched systems," *IEEE Control Systems*, vol. 19, no. 5, pp. 59–70. Oct. 1999.

[12] L. E. Parker, "Current state of the art in distributed robot systems," *Distributed Autonomous Robotic Systems 4*, L. E. Parker, G. Bekey, and J. Barhen (eds.), Springer, pp. 3–12, 2000.

[13] D. Stilwell and B. Bishop, "A framework for decentralized control of autonomous vehicles," *Proc. IEEE Int. Conf. Robot. Automat.*, San Francisco, CA, April 2000, pp. 2358–2363.

[14] H. Yamaguchi and J. W. Burdick, "Asymptotic stabilization of multiple nonholonomic mobile robots forming groups formations," *Proc. IEEE Int. Conf. Robot. Automat.*, Leuven, Belgium, May 1998, pp. 3573–3580.